Monte Carlo studies for medical imaging detector optimization

Monte Carlo studies for medical imaging detector optimization

G R Fois[1,2]**, E Cisbani**[2]**, F Garibaldi**[1,2]

[1] Istituto Nazionale di Fisica Nucleare (INFN), sezione di Roma, Piazzale Aldo Moro 2, 00181 Roma

[2] Istituto Superiore di Sanità (ISS), viale Regina Elena 299, 00161 Roma

E-mail: `giovannarosa.fois@gmail.com`

Abstract. This work reports on the Monte Carlo optimization studies of detection systems for Molecular Breast Imaging with radionuclides and Bremsstrahlung Imaging in nuclear medicine.

Molecular Breast Imaging requires competing performances of the detectors: high efficiency and high spatial resolutions; in this direction, it has been proposed an innovative device which combines images from two different, and somehow complementary, detectors at the opposite sides of the breast. The dual detector design allows for spot compression and improves significantly the performance of the overall system if all components are well tuned, layout and processing carefully optimized; in this direction the Monte Carlo simulation represents a valuable tools.

In recent years, Bremsstrahlung Imaging potentiality in internal radiotherapy (with beta-radiopharmaceuticals) has been clearly emerged; Bremsstrahlung Imaging is currently performed with existing detector generally used for single photon radioisotopes. We are evaluating the possibility to adapt an existing compact gamma camera and optimize by Monte Carlo its performance for Bremsstrahlung imaging with photons emitted by the beta- from ^{90}Y.

1. Introduction

Medical imaging is a field of research in continuous development. This sector is of fundamental importance for the early diagnosis and treatment of many diseases. Medical imaging includes a whole series of techniques, very different from each other, whose common purpose is to make visible the interior structures of the body. Nowadays various techniques are in use, such as: radiography, which is among the most common tests for the study of the skeletal system, the CT (Computed Tomography) that allows to obtain three-dimensional images. In the field of nuclear medicine is worth cite the PET (Positron Emission Tomography) which provides physiological information through maps of functional processes within the body. There are also a number of imaging techniques that do not make use of ionizing radiation such as ultrasound, which exploits the transmission of the ultrasonic waves, and MRI (Magnetic Resonance Imaging), which is a technique of image generation based on the physical principle of nuclear magnetic resonance.

In this broader context we focused our attention on two molecular imaging techniques based on single photon detection: MBI (Molecular Breast Imaging) and BSI (Bremsstrahlung Imaging).

1.1. MBI

Breast cancer is one of the most common cancers in women. Early detection and improved diagnosis lead to more efficient treatment and better outcomes. Mammography is the current gold standard for early breast cancer detection. Mammography is typically very sensitive but not specific. In addition, his sensitivity is significantly reduced in certain subset of women, particularly in women with radiographically dense breasts. As a result, majority of mammography-directed biopsies are performed on benign lesions and a significant number of biopsies are therefore unnecessary. Recognizing the limitation of mammography, additional adjunct diagnostic methods need to be applied. Among them molecular imaging with radionuclides has a central role to play.

MBI is a nuclear medicine technique that provide high-resolution functional images of the breast. MBI have as their origin an older technique called scintimammography which used conventional γ-cameras to image the uptake of Tc-99m sestamibi in breast tumors. Because of the large dead space at the edge of the camera requiring the patient to be imaged prone with the camera positioned laterally, the resulted distance between the breast and the camera increased leading to a considerable loss of resolution [1]. So the standard γ-cameras initially used do not offer sufficient spatial resolution to detect small lesions when used in breast imaging scintimammography procedure. O'Connor et al. [2] studied a dual-head system which allows simultaneous acquisition of superior and inferior views of the breast. Thanks to the use of such dual-head MBI system, a significantly increase sensitivity for subcentimeter lesions was found.

Our group has designed and implemented a dual detector layout which consists of two detectors of different dimensions: a 150×200 cm^2 with parallel hole collimator the first, and a 7×7cm^2 with pinhole collimator the second. This asymmetric setup allows monitoring the whole breast and performing spot compression bringing the detector closer to the potential suspicious lesion therefore increasing the efficiency and at the same time imaging it with relatively high resolution thanks to the pin-hole magnification [3].

1.2. BSI

The effective use of radionuclides in cancer treatment such as TRT (Targeted Radionuclide Therapy) requires the knowledge of their spatial and temporal distribution on a personalised base. The use of beta-emitters radionuclides has been proposed as a means of enhancing the dose deposition within the targeted cells while minimizing the dose received by other organs. The Bremsstrahlung interactions of the emitted beta in the body produces a continuous spectrum of photons that can be used for imaging the beta-radiopharmaceuticals distribution. [4].

Our work aims to investigate the Bremsstrahlung imaging with compact gamma cameras and identify the best procedures and solutions to maximise its quality.

2. Materials and methods

This Monte Carlo study has been carried out using the GATE simulation code. GATE is an advanced opensource software developed by the international OpenGATE collaboration and dedicated to numerical simulations in medical imaging and radiotherapy [5].

In the simulations we have implemented the geometries of our experimental setups.

MBI system consists of a large detector which has the same dimension as a standard mammographic screen (150×200mm^2), and a smaller one with dimension allowing spot compression (70×70mm^2). Both detectors have been implemented in the simulation.

The first detector uses a 1 cm Tungsten parallel hole collimator with 1 mm holes and 0.34 mm septa. A 0.5 mm of Al is positioned right after the collimator coating a 6 mm layer of NaI, and a layer of 3 mm of glass coupled the scintillator to the photodetector.

The second detector has a 4 mm Tungsten pinhole collimator with a 2 mm hole. The NaI layer is placed 38 mm from the collimator. The image obtained with pinhole collimator has

a certain magnification due to the detector geometry itself. The magnification factors have been calculated for different distances of the source from the collimator, and a processing of the simulated image was done taking into account those magnification factors to normalise the image in order to fuse it with the parallel hole one.

The detectors are placed in an opposite position one to each other and a 5 cm water phantom is placed between them.

GATE code permits to simulate the scintillation process of gammas from the source inside the scintillation layer. The optical photons generated are followed simulating their interaction processes inside the detector volume and their last position at the end of the glass layer is recorded.

An analysis code allow to study the simulation output and, taking into account the quantum efficiency of the photodetector, to reconstruct the position of the gamma from his optical photons generated and so to construct an image of the source.

The ^{99}Tc emission is simulated by a monochromatic source of 140 keV in energy.

For BSI we used the same detector as implemented in MBI changing some parameters of parallel hole collimator. In this case the collimator was a 20 mm Tungsten slab with 1.475 mm^2 hole dimension, and 0.305 mm septum dimension. An ^{90}Y source has been implemented.

3. Results

3.1. MBI

A monochromatic point source was used to determine the spatial resolution of the system. The following table shows the results of spatial resolution obtained for the two detectors for different distances of the source.

Table 1. Spatial resolution calculated from the simulations.

Source/Collimator distance	SR (mm) Parallel hole	Analytical values	SR (mm) Pinhole	Analytical values
1.0 cm	3.7	3.1	2.6	1.7
1.5 cm	4.0	3.7	2.8	2.0
2.0 cm	4.6	4.4	3.1	2.1
2.5 cm	5.1	5.0	3.3	2.2

The values of spatial resolution obtained are in good agreement with the analytical values calculated.

The intrinsic resolution of the crystal has been estimated using a directional source. The treatment at the interface has been taken into account. We determine the intrinsic resolution depending on the reflectivity or absorbant properties at the entrance and at the lateral walls of the crystal.

Every images was obtained simulating a background and an hotspot. The background source had the same dimension as the water phantom. The hotspot was a sphere with variable dimension in a range between 3 mm to 5 mm radius, and was placed in the middle of the phantom at different distances from the detectors: from 10 mm to 25 mm distance from the pinhole, and from 40 mm to 25 mm from parallel hole collimator respectively. The uptake used in this work was 10/1.

Images obtained with both detectors have been processed and a combined image was obtained by pixel to pixel values multiplication after proper normalisation.

Table 2. Intrinsic resolution of the crystal respect to inner wall coating of it.

Spatial resolution	Lateral walls	Entrance
1.15 mm	reflective	reflective
0.82 mm	absorbant	reflective
0.82 mm	70% absorbant	10% absorbant

The SNR (Signal to Noise Ratio) has been used to characterize the image. SNR values obtained are shown for different hotspot sizes.

Table 3. SNR estimated values for different hotspot radii.

Hotspot r = 5 mm

Dist. (mm)	Par	Pin	Combo
10/40	21	50	60
15/35	24	56	66
20/30	24	46	56
25/35	30	37	49

Hotspot r = 4 mm

Dist. (mm)	Par	Pin	Combo
10/40	10	36	37
15/35	13	38	42
20/30	15	31	35
25/35	19	27	31

Hotspot r = 3 mm

Dist. (mm)	Par	Pin	Combo
10/40	5	23	24
15/35	6	23	24
20/30	7	21	21
25/35	10	20	21

As is shown by the simulations, the use of a pinhole collimator allowing spot compression, which means that the detector can be positioned closer to the lesion, leads to a greater SNR values in the combined image and hopefully to a major detectability of smaller lesions.

3.2. BSI

We simulated a spherical beta-emitting source, 3 mm radius, positioned inside a water phantom. The Bremsstralung interaction positions were recorded to study the origin of the detected Bremsstrahlung gammas. In figure [1] a 3D map of Bremsstrahlung events distribution is shown as well as the events distribution along an axis. The events distribution results in a FWHM of about 9 mm for a spherical source of 6 mm in diameter.

As before, the image was reconstructed from the optical photons generated by the interaction of Bremsstrahlung photons with the scintillation material. In the upper part of figure [3] an example of reconstructed image is shown. A study in energy was performed, reconstructing images in different energy windows. At higher energy the directional information carried by the photon is compromised by the relative transparency of the collimators and the reduced photon absorption of the detector walls. On the other hand, low energy Bremsstrahlung photons still carry on direction information and actually provide clean, well contrasted, images.

The Monte Carlo results were preliminary compared to real data, obtained by two phantoms composed by Perspex cylinders with three small cylindrical cavities each, loaded with a ^{90}Y solution. As shown in figure [2], one cavity is on the axis of the phantom, a second one is close the axis and a third cavity is near the phantom border.

The image acquired experimentally was studied as function of the energy. As for the simulation study, a very informative image resulted for lower energies as shown in the lower part of figure [3].
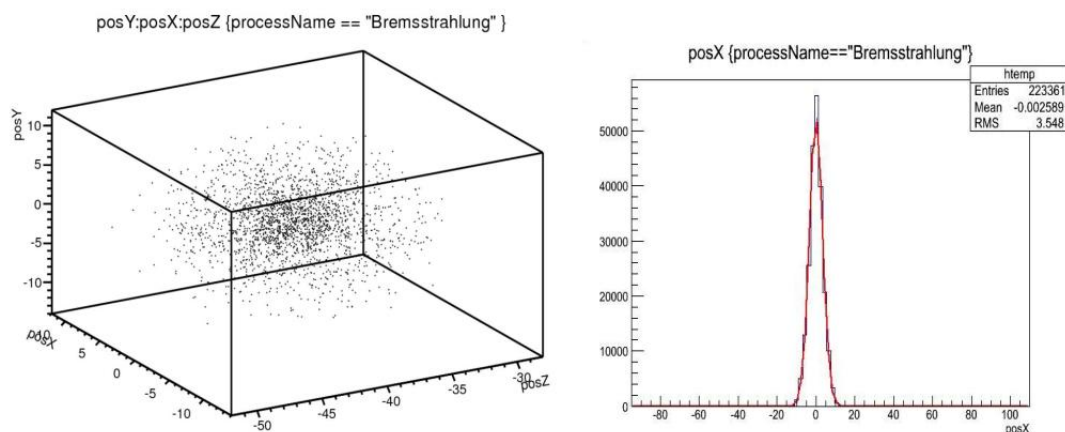
Figure 1. Left: Bremsstrahlung events distribution inside a water phantom. Right: Bremsstrahlung events distribution along an axis.
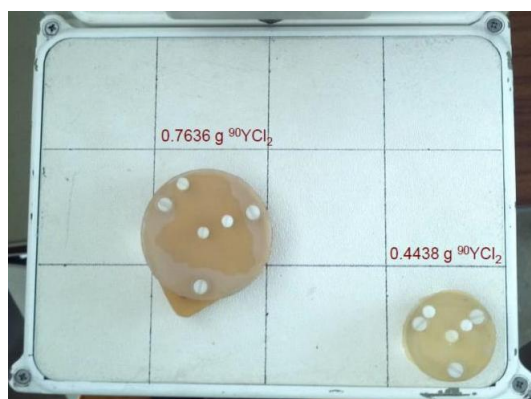

Figure 2. The two Perspex cylinders used in the experiments.

4. Conclusions

4.1. MBI
A good agreement between analytic calculation and simulated data as been obtained, somehow validating the Monte Carlo approach. The SNR of the properly combined image from the two detectors is noticeably better than the SNR of the single images; this will enhance the detection probability of small lesions, without affecting significantly the spatial resolution.

4.2. BSI
This preliminary study confirms the possibility to trace a beta emitter through Bremsstrahlung gammas. A compact gamma camera was adapted for Bremsstrahlung photon imaging and indirectly beta- distribution monitoring; real data have been acquired by a more complex system however results are in good qualitative agreement with the simulated Monte Carlo simplified model.

Further analysis work is necessary to complete the Monte Carlo studies, however the implemented model and procedures are flexible enough to permit the study of the response of a quite extended potential applications such as MBI and BSI.
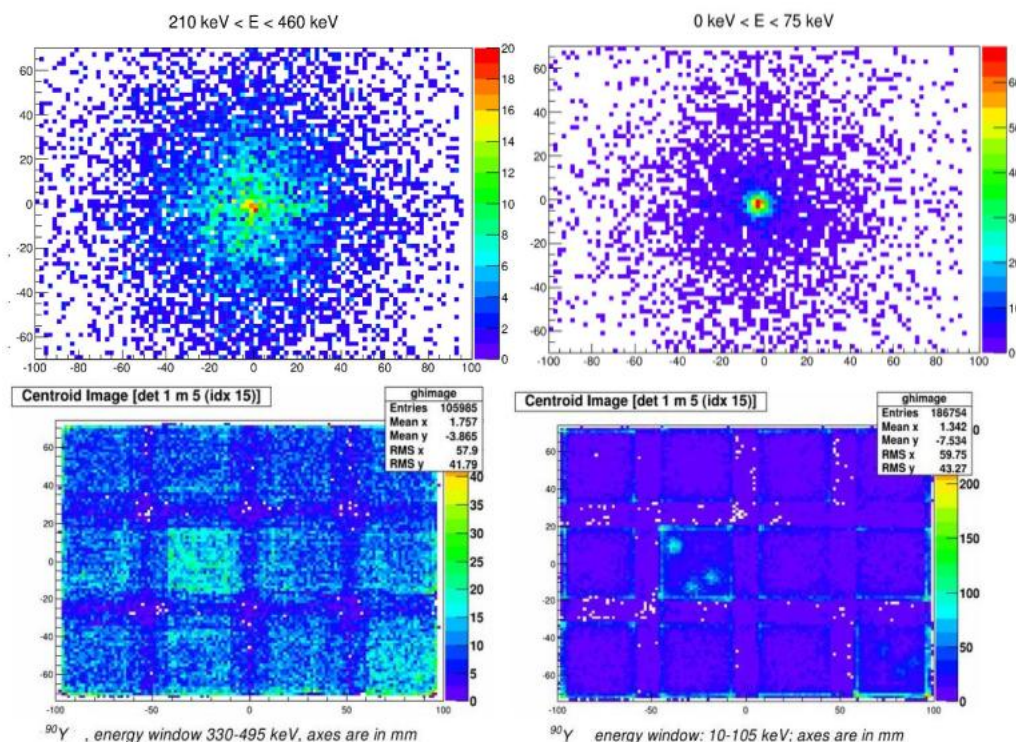
Figure 3. Top: simulated images from a spherical source 6 mm diameter, with different energy cuts: the lower energy photons provide the best image. Bottom: images of real phantoms with approximately the same energy cuts of the corresponding simulated images.

References
[1] O'Connor M, Rhodes D, Hruska C 2009, *Expert Rev Anticancer Ther*, 9(8): 1073-80
[2] Hruska CB, Phillips SW, Whaley DH, Rhodes DJ, O'Connor MK 2008, *AJR Am J Roentgenol*, 191(6): 1805-15
[3] Cusanno F, et al. 2007, *Nuclear Instruments and Methods in Physics Research A*,**571**, Issues 1-2, 77-80
[4] Shen S, DeNardo L, Yuan A, DeNardo DA, DeNardo SJ, 1994, J Nucl Med,**35**, no. 8, 1381-89
[5] Morel C, et al., 2004, Phys Med Biol,**49**, Pages 4543-61
[6] G. Ponti et al., Proceedings of the 2014 International Conference on High Performance Computing and Simulation, HPCS 2014, art. no. 6903807, 1030-33